

A Combined Atomic-Resolution STEM and First-Principles Approach Towards Understanding the Origins of the First Solar-System Solids

T.J. Zega^{1,2}, V. Manga^{1,2}, K. Watanabe³, K. Domanik¹, P. Mane¹, A. Hanawa³, H. Inada³, J.Y. Howe⁴, K. Muralidharan²

¹ Lunar and Planetary Laboratory, University of Arizona, Tucson, U.S.A.

² Dept. of Materials Science and Engineering, University of Arizona, Tucson, U.S.A.

³ Hitachi High Technologies Inc., Hitachinaka, Japan

⁴ Hitachi High Technologies America Inc., Clarksburg, U.S.A.

Introduction: Primitive chondritic meteorites contain mm- to cm-sized assemblages of Ca- and Al-bearing oxides and silicates. So-called calcium-aluminum-rich inclusions (CAIs) have radiometric age dates of 4.5673 Ga, exceeding those of all other solar-system materials [1]. Moreover, equilibrium thermodynamic calculations show that the materials within CAIs formed at very high (>1300 K) temperatures [2]. Analysis of these objects can therefore provide insight into chemical and physical processes that occurred in the early solar system. Perovskite, nominally CaTiO₃, occurs within primitive CAIs. It is the major Ti-bearing phase in these refractory inclusions, and is thermodynamically predicted to condense at 1593K [2]. We examined perovskite structure and composition down to the atomic level to better understand the thermodynamic conditions in which these refractory materials formed.

Samples and Methods: Plan-view petrographic thin sections of Allende, Axtell, and NWA 5028 chondrites were examined for perovskite grains. We acquired secondary and backscatter electron images of the CAIs as well as elemental maps using the Cameca SX-100 electron microprobe and the FEI Helios focused-ion-beam scanning electron microscope (FIB-SEM) at the University of Arizona. Several perovskite grains were selected for detailed investigation and were extracted on the Helios and thinned to electron transparency using previously described methods [3]. All samples were ion polished to 5 keV to remove the amorphous damage layer created by higher-voltage milling. We analyzed all sections using the newly developed 200 keV Hitachi HF5000 scanning transmission electron microscope (S/TEM) located at Hitachi Hi-Tech (Hitachinaka, Japan) as well as with the newly installed HF5000 located at the University of Arizona. The HF5000 is equipped with a cold-field-emission gun, a Hitachi 3rd-order aberration-corrector for scanning TEM (STEM) imaging, a twin Si-drift Oxford EDS system, and a Gatan Quantum ER imaging filter (GIF) for electron energy-loss spectroscopy (EELS). We also performed first-principles density-functional theory (DFT) calculations to predict grain structure and chemistry for comparison to our experimental data.

Results and Discussion: STEM imaging shows that all FIB sections are all polyphasic and the perovskite grains hosted within them range in size from nm to several μm. A perovskite grain from Allende FIB section 'C' contains a spinel inclusion ~300 × 400 nm in size. We used atomic-resolution STEM imaging to probe the spinel structure further. The HF5000 was operated in STEM mode (30 μm STEM aperture) using the HR mapping setup (~100 pm probe and 50 to 100 pA current). HAADF imaging shows that the spinel is twinned along the [111] direction, and the contrast at the boundary is, on average, higher Z than the adjacent bulk crystal (Fig. 1a). To determine the identity of the higher-Z material, we performed EDS mapping with a resolution of 128 x 128 px, a dwell time of 2.85 ms, and a process time of 6 in the Oxford software. EDS spectrum images suggest that the twin boundary contains V, whereas the adjacent bulk crystal contains Mg, Al, and O (Fig. 1a). However, because of the overlap

of the V and Ti $K\alpha$ X-ray lines, we tested for the presence of V using EELS. We acquired EELS spectrum images over an area measuring ~ 6.7 nm \times 1.34 nm using an entrance aperture of 5 mm, a drift-tube offset of 420 eV, a dispersion of 0.1 eV/ch, a 0.12 nm pixel size, and an integration time of 0.2 s. EELS spectrum images confirm V at the twin boundary, whereas O occurs in the adjacent bulk crystal but is relatively lower signal at the twin boundary.

To complement our aberration-corrected imaging, we performed DFT calculations to better understand the atomic structure of the twin boundary and the role that V plays. Supercells with 336-atoms (Fig. 1b) were used for calculation of (111) twins in the spinel, with and without V. The formation of a (111) twin leads to distortions in O-bearing octahedral and tetrahedral units in its vicinity. While undistorted O-bearing octahedra in spinel exhibit a single Al-O distance of 1.94 Å, the distorted O-octahedron exhibits two different Al-O distances of 1.97 Å and 2.05 Å. Similarly, O-tetrahedra near the (111) twin exhibit two Mg-O distances of 1.80 Å and 1.94 Å instead of a single Mg-O distance (1.96 Å) that was measured in the pristine bulk structure. First-principles calculations predict a (111) twin formation energy of 473 mJ/m² in the pure spinel phase. In comparison, the calculations show that if V substitutes Mg near the twin, by 16% of the total Mg sites, the twin formation energy in the spinel is reduced to 441 mJ/m². *The segregation of dissolved V in the spinel at the (111) twin boundaries is therefore thermodynamically favorable.* These results explain the thermodynamic driving force for V-decorated (111) twins in the spinel phase as observed in C_s-corrected STEM measurements.

To our knowledge, this is the first observation of atomic V segregation to a twin boundary in meteoritic spinel hosted within a perovskite grain. Its presence has important implications for the thermodynamics of the system in which these refractory materials formed, and we will discuss these at the meeting. Nonetheless, aberration-corrected imaging of planetary materials can reveal new chemical information on solar-system formation, and first-principles calculations can help provide new fundamental insights into the energetics and thermodynamics of the origins of these important materials.

References:

- [1] Connelly J. N. et al., *Science*, 338, (2012), p. 651-655.
- [2] Lodders K. (2003) *Astrophys. J.*, 591, 1220-1247.
- [3] Zega T. J. et al. *Meteoritics & Planet. Sci.*, 42 (2007), 1373-1386.
- [4] We thank Jose Jimenez for install and setup of the HF5000 at the University of Arizona. Research supported by the UA Office of Research, Discovery, and Innovation in conjunction with NSF grant 1531243 and NASA grants NNX15AJ22G and NNX12AL47G.

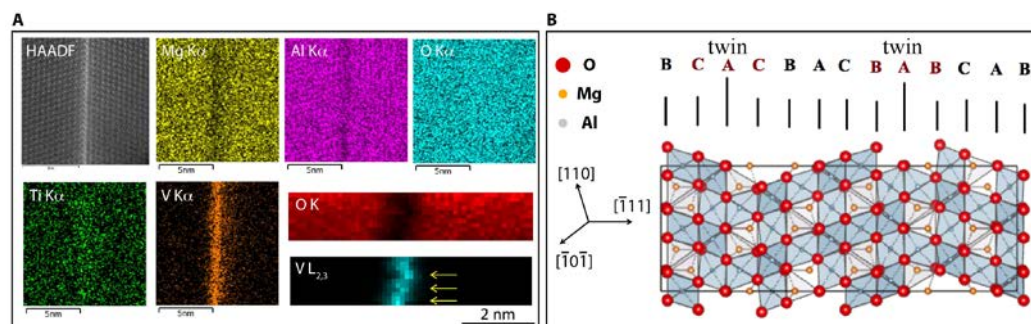


Figure 1. (A) TEM data on spinel from Allende FIB section 'C'. (B) Energy-minimized twin structure from DFT calculations.